Advanced BCI

Angeliki-Ilektra Karaiskou, Robert Reichert, Veerle Schepers

June 2019

Contents

1 Introduction

1.1 Motivation of the Problem

Diseases of motor neuron system like Amyotrophic Lateral Sclerosis (ALS) cause the progressive cell death of the peripheral neurons controlling muscle contraction [17]. As a consequence, normal muscular and cognitive functioning can decrease to the point where even basic human interaction becomes impossible. Similarly, other medical conditions exist that can lead to a restriction in muscular movement or the ability to communicate. Brain stem damage can cause patients to be in a locked in state. Neuromuscular dystrophy, spinal muscular atrophy, several brain tumors and other progressive diseases like Huntingtons disease or multiple sclerose in its final stages might lead to sever disabilities involving the loss of muscle and speech functions.

In all of those cases, technology-based interventions can increase the freedom of interactions and communication for patients. Augmentative and Alternative Communication Technology (AAC) like the Freedom 2000TM Toughbook are established and accepted means of communication [1]. Eye tracking technology and its potential for human computer interaction is another established mean used to facilitate communication and interaction with software. Here, efforts are even made to combine the technology with everyday applications like the in-built iPad camera [14]. With advancement in neurotechnology and increasing knowledge of brain functions, the application of Brain Computer Interfacing (BCI) becomes another realistic tool to aid patients. Here, they can use the brain to communicate and control external devices. In contrast to the aforementioned technologies, BCIs offer a wide variety of signal signatures to be extracted and utilized. Even though the signals derived from electromagnetic volume conduction captured trough electroencephalography (EEG) are small and noisy, the potential of the variability might overthrow competing technologies like eye tracking as a means of restoring communication. Examples where the high variability of brain signals are useful can be demonstrated by totally locked-in patient groups. Here, patients lost control over their extra-ocular muscles. Nevertheless, they are still able to voluntary control other brain signals like imagined movement or covert attention [23] in many cases.

BCI technology can enable wheelchair bound patients to navigate, communicate and control basic functions within their environment. Moving around, sending specific SOS notifications, contacting peers and controlling a television are only a few examples where a small variety of options under the control of a patients can potentially increase the autonomy and quality of life for patients tremendously. To facilitate such optionalities, current BCIs require an interface where patients are able to distinguish between several choices. Current BCIs use a variety of signals like: e.g. imagined movement [15], auditory steady state evoked potential (ASSEP) [12] or other evoked paradigms like the P300 and/or N100 [22]. Comparing the quality and achieved accuracies of the above mentioned signal sources we focused on an visual paradigm. The human visual stream provides many advantages like high classification accuracies that other BCI paradigms cannot provide.
Among event related potentials the P300 has been successfully and robustly implemented for many BCI applications [19] [5]. The P300 is a positive evoked potential around 250 ms to 500 ms after stimulus onset mostly associated with an individuals reaction to an oddball stimulus[20]. Even though the P300 is robust and reliable, its time structure also upper-bounds the speed in which individual can make choices between different decision classes. Due to this limitation, we focused on a steady state visual evoked potential (SSVEP) paradigm as our choice of a visually detectable brain signal. Here, high the variability of signal signatures allow for many classes of choices combined with fast choice making.

1.2 Our Original Idea

Research about combining SSVEP based BCIs with navigating a wheelchair has already been conducted [15] [21]. Here, different teams of researchers used different brain signals like imagined movement to facilitate distinctive tasks. Patients using our BCI should be able to execute the different tasks by mainly using the reliable SSVEP response. In addition, they should be able to use imagined movement to navigate so that their vision is unimpeded during navigation by the screen. On top of this alpha wave frequencies evoked through relaxation were planned to be utilized to switch between menus.

2 Methods

2.1 Materials

The BCI system is programmed in Matlab with the psychtoolbox extension to achieve better temporal resolution. The scripts run on a windows computer and are shown to the subject on a display with a refresh rate of 60 Hz.
The EEG is recorded using a portable 32 channel system, with the electrodes individually placed on the cap according to the international 10–20-electrode system. The ground electrode was placed on the left arm with a wristband.

2.2 Subjects

Three healthy subjects (2 female, 1 male), with a mean age 25.6 years (ranging from 24 to 28) participated in this study. All where neuroscience students at the Radboud University Nijmegen and had normal or corrected to normal vision. All participants where aware of the use of flickering stimuli and confirmed that they had never suffered from epilepsy.

2.3 Interface Design

The BCI needs to be able to perform four distinguished tasks with different sub-tasks, namely moving a wheelchair in four directions, calling three different people, sending three different emergency messages, and changing the TV to three different channels. Putting all these different options in one screen would cause a very busy screen which could lead to overloading when people are using it. Therefore, we choose to design a main screen where you can choose between the four different tasks, and sub-menus for each of these tasks to choose from the available options within this menu. Besides overcoming overloading, this makes it also easier to allow for additional options within each menu, or even adding new tasks. For safety reasons and convenience for the user we decided that the SOS menu should be directly accessible from the main menu, as well as from each of the sub-menus.

As discussed above, the initial idea was to make a BCI that makes use of both brain oscillations at different frequencies and imagined movement.
Since the discovery of the Alpha waves in 1929 by Bergen, they are assumed to be related to a state of closed eyes [10]. Alpha waves, typically ranging between 8 and 12 Hz, are most prominently found in the occipital cortex [26]. Since Alpha waves also appear unintentionally when people are just closing their eyes to relax, it would be a bad idea to assign them to a certain task. Therefore, we decided to try and use Alpha waves to go back from each of the sub-menus to the main menu. Furthermore, when someone just falls asleep and wakes up again, being in the main menu is more convenient than to be in any other menu.

For selecting the tasks from the main menu, and the options within each tasks from the sub-menus we decided to use steady state visual evoked potentials (SSVEP).
SSVEP can be explained as the fact that when a person attends (either cover or overt attention work) to a flickering stimulus with a constant frequency, this evokes a brain oscillations in the visual cortex with peaks at the fundamental frequency of the stimulus, as well as on the harmonics of this frequency [16, 31]. The idea here would be to show a block for each of the menu options, and each of them is flickering at a different frequency. The user is then instructed to attend to one of the blocks, which will create brain signals at the corresponding frequency. These local oscillations are transmitted via volume conduction through brain matter, bone and skin and can be measured with an EEG device, which can be used to select the corresponding option.

Attending to these flickering blocks comes with the cost of not being able to attend to the environment as much as before. When you are selecting a TV channel, calling someone or sending an SOS message, this is not a big problem. However, while driving around in the wheelchair this could become problematic. Therefore, we want to use imagined movement to select in which direction you want to go while being in the movement menu.

Although there are clear reasons to use Alpha waves and imagined movement, this also introduced some considerations. As discussed above, the signals for imagined movement can be hard to catch, and the alpha signal might be hard to distinguish from the frequency of the blocks, or the noise. Tackling all these issues at once seems like a rather challenging task, and therefore, in our final design for this BCI we decided to go with a simplified version, that could later be extended to our original idea.
In this simplified design, we get rid of both the alpha waves and the imagined movement, which are replaced by additional flickering blocks. Since we are using the main- and the sub-menus this still doesn't cause overloading, since a maximum of 6 blocks are present on the screen at each time. Using these additional flickering blocks also makes it possible to add additional option when extending the design in the future. All options are thus selected via SSVEP and this makes it even more important to utilize optimal stimuli parameters, meaning that the brain signal response to the blocks should be maximized to be able to easily detect and distinguish them. To do this we focus on three properties. First we investigate which flickering frequencies should be used.

Secondly, we study the effect that different colors of, as well as the contrast between the stimuli and background can have. Finally, we also take the size and positioning of the blocks into account.

2.3.1 Frequencies

To select the most optimal frequencies we have to take two main things into account. The first is how the brain, and more specifically the occipital cortex responds to certain frequencies, and secondly what frequencies could be produced with the hardware we use.
Most currently used computers, and also the one we used have a refresh rate of 60 Hz. This means that a bock is either visible or invisible for at least a period of $\frac{1}{60}$ sec. The frequency comes about as $\frac{1}{t}$, where t is the time of a full cycle in seconds. A full cycle means that the stimulus needs to be both turned on and off at least once. The maximum flickering frequency is achieved with the shortest cycle, which would be achieved by turning the block off for one screen, and off for the next one. This means that we get the minimum period of $t = \frac{1}{60} + \frac{1}{60} = \frac{1}{30}$ sec, and accordingly we get maximum frequency that could be created with this system at 30 Hz. The minimum frequency is achieved by the longest period, and thus by the recording time. If we use a recording time of 4 sec. this would mean that we can achieve a frequency of $f = \frac{1}{t} = \frac{1}{4} = 0.25$ Hz. Frequencies in-between can be achieved by creating cycles of $\frac{x}{60}$, where x is an integer and $\frac{1}{30} < x < \frac{1}{4}$. Table 1 shows the 15 highest possible frequencies that we can create based on their on-off cycle and their according periods.

cycle	t	f
0-1	0.03	30
0-0-1	0.05	20
0-0-1-1	0.07	15
0-0-0-1-1	0.08	12
0-0-0-1-1-1	0.10	10
0-0-0-0-1-1-1	0.12	8.571428571
0-0-0-0-1-1-1-1	0.13	7.5
0-0-0-0-0-1-1-1-1	0.15	6.666666667
0-0-0-0-0-1-1-1-1-1	0.17	6
0-0-0-0-0-0-1-1-1-1-1	0.18	5.454545455
0-0-0-0-0-0-1-1-1-1-1-1	0.20	5
0-0-0-0-0-0-0-1-1-1-1-1-1	0.22	4.615384615
0-0-0-0-0-0-0-1-1-1-1-1-1-1	0.23	4.285714286
0-0-0-0-0-0-0-0-1-1-1-1-1-1-1	0.25	4

Table 1: The 15 shortest possible cycles with their according period and frequency for a computer with a refreshing rate of 60 Hz.

The brain is thought to be able to handle a wide range of frequencies. The strength depends on the frequencies itself, and on the anatomical location.
These differences in response strength to different frequencies is related to the number of neurons involved. First of all, how many neurons are involved is dependent on the synchronization between neurons. Neuronal oscillation synchronization can be described by the Kuramoto model. Simplistically seen, this model states that each oscillator (neuron) has its own preferred frequency, but is biased by the interaction with other oscillators and their frequencies [3, 7]. Whether or not neurons eventually become synchronized further depends on the "band-pass filter" theory of neuronal signal transfer [31]. Here, the "all or none" firing property of the axon hillock effectively creates a low pas filter. If the stimulus frequency is to high, new signal input arrives within the refractory period of the neuron and does not create another action potential. In addition, the chemical properties of the chemical synapses depend on the frequency of the stimulation as

well. Here, infrequent stimulation results in a low chemical density of neurotransmitters which are unable to activate the postsynaptic neuron, albeit creating a high- pass filter.
A research investigating the brain responses to a flickering light at frequencies from 1 to 100 Hz (step-size 1 Hz) found that the visual cortex shows synchronizations up to at least 50 Hz [11]. Several researches report strongest brain responses in the visual cortex for synchronization to stimuli in the Beta range (14 - 30 Hz), of which some of them also report strong responses to stimuli in the Alpha range (9 - 13 Hz) [6, 13, 25].
Based on these findings we would prefer to use frequencies in the Beta range, however, we still need to take our hardware limitations into account. Based on this 30, 20, 15, 12, 10, and 8.5 Hz. Another thing we need to take into account is the harmonics of the frequencies we use. For example, we can expect to see a harmonic at 15 Hz for the 30 Hs stimulus and at 20 Hz for the 10 Hz stimulus [11]. The harmonics can have both more or less power then the presented frequency itself. This effect can partly be explained by with the Planck's equation, which states that the amount of energy is dependent on the frequency. Lower frequencies have more oscillations within the same period as higher frequencies, which makes the reason why lower frequencies have higher energy more obvious Cooray2008. Due to this higher energy at lower frequencies it thus is possible to get a higher peak at the lower harmonic of your stimulus. However, the full response of e.g. a 15 Hz and a 30 Hz will still look different and therefor they can still be differentiated from each other when using a classifier does not look for the highest peak, but rather tries to match the full response.

2.3.2 Color and contrast

The color of the background and the stimuli, as well as the contrast between them could possibly have a great influence on the accuracy of the BCI system. To decide which colors to use we need to take into account how humans process color.
The colour encoding cone cells of the human retina are only sensitive to three different wavelengths: blue, green and red, as described in the trichromatic theory of colour vision [4]. Ganglion cells relay the cone stimulated signalling via colour opponency in a relative, rather than absolute manner [24]. Hereby, it is informative to realize that the three ganglion pathways (magnocellular, parvocellular and koniocellular pathway) differ in size and proportion within the layers of the cortex. Hence, we believe maximum flickering read out at the visual cortex can achieved through maximizing colour opponency of the biggest ganglion pathway. Those are magnocellular ganglion cells encoding dark and bright contrast which has implication for our colour stimulus design. The biggest contrast exist between black and white, which thus is expected to create the strongest signal.
Aesthetically it would be more convenient to use blocks of different colors. Another reason to consider using different colors is to minimize interference of different blocks. However, interference does not seem to be a big problem. Ordikhani-Seyedlar instructed subjects first to overtly attend (by shifting the eyes) to one of two flickering blocks, and later he instructed them to look at a cross in-between the two blocks while covertly attending (shifting the mind) to one of the two blocks [18]. He found that even with covert attention brain oscillations only synchronized with the frequency of the block that the subject was currently attending to. Thus, colored blocks are not necessary to overcome interference. Although aesthetically it still might be better to use colored blocks, the attenuation of signal quality due to reduced contrast remains more important. Therefore, we choose to use white blocks for all the stimuli.

2.3.3 Position and size

Moreover, the distribution of a projection of foveal retina cells can be quantified through retinotopic mapping. Hereby, a few degrees of vision on the retina take up large amounts of the visual cortex, which is relevant for electrode choice and stimulus size in the finalized BCI [27]. In general, the bigger the stimulus size, the bigger the amplitude of the response on the occipital cortex [8]. However, the greater the stimulus size, the greater the possible discomfort due to the maximized

colour contrast and the constant stimulation. Visual fatigue seems to induce performance decrease [**Lee2018**]. Hence, we decided to use a stimulus which displayed on typical screens exceeds a visual angle exceeding 5 degrees at 80 cm distance. The precise values can be obtained using the formula:

$$visual\ angle = 2 \cdot atan \frac{\frac{object\ size}{2}}{object\ distance} \tag{1}$$

How the blocks are arranged on the screen is dependent on several factors. First of all, on the grounds that we want to make the blocks as big as possible to get the strongest brain signals. Secondly, the blocks should be positioned in a congruent way, e.g. the block for turning left should not be on the right side of the block for turning right. Finally, we also take into account the aesthetics of the system. Based on these considerations we looked at the different menus. The movement menu has the maximum amount of blocks on the screen, and it also can cause the most confusion if blocks are arranged incongruently. Thereupon we decided to take this screen as a starting point to arrange the blocks and to keep the system as constant as possible over the different menus we arranged the other menus accordingly.

The movement menu consists of the four block to move the wheelchair in each direction, the block to go back to the main menu, and the block to go to the SOS menu. It is most convenient of the options for this menu, moving around, are separated from the other two blocks. When looking at currently used BCIs for people that use a wheelchair, most of the systems are placed on the persons right hand side. Accordingly the left side of the BCI screen is positioned more in the center of view than the right side. Based on this we made the decision to put the menu-dependent blocks on the left side of the screen, and the back and SOS button on the right side.
The BACK and SOS buttons are positioned in the corners to separate them as far as possible from the other blocks to make it easier to attend to them. The movement buttons are positioned according to the direction to move in.

All other menus are designed to be maximally consistent with the movement menu. Thus, the back and SOS button (if present in the screen) are always shown in the right top and bottom corner. The menu-dependent blocks are always on the left side, and always position in the same way as the movement menu, again to keep the menus consistent. If the other menus only have three options to choose from, thus the lowest block is removed. We choose to remove this block since this is also the block that is less used in the movement menu.
Putting all our considerations together we designed the different interface menus as shown in image 1.

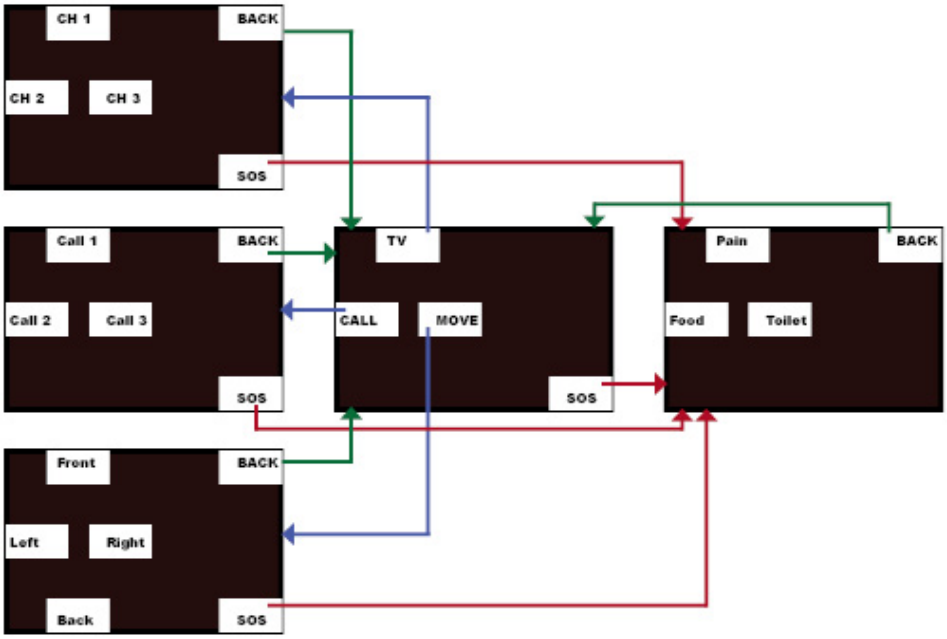

Figure 1: Interface Pipeline

2.4 SSVEP Identification

An SSVEP response is characterized by the stimulus central frequency and its harmonics. For that reason, one of the most used feature extraction techniques is the Power Spectral Density (PSD) analysis by using the FFT of a sliding window with a specific length[2]. However, since the FFT is susceptible to noise, new approaches are investigated. Among them, Multivariate Linear Regression (MLR)[28] seems to be a robust and successful technique for the recognition of the different flickering frequencies.

2.4.1 SSVEP Identification based on MLR

The logic behind MLR is simple : combine the recordings in respect to their channel, reduce the dimensionality of the feature vector with Principal Component Analysis (PCA) and create the weight matrices based on MLR by minimizing the sum-of-squares cost function. Let

$$X = [x_1, ..., x_N] \in \mathbb{R}^{D \times N} \tag{2}$$

be the EEG recordings, with

- D is the feature dimensionality ($D = C$ channels $\times T$ temporal points)
- N is the number of training trials
- $D > N$, in BCI recordings

The number of different classes, different stimulus frequencies, is denoted by F.

Because the dimension of the data is big in comparison to the different trials, PCA is used in order to reduce it. In order to extract the PCA features a variance normalization is first required. Then, the principal components which have at least the 99% of the whole data variance are chosen. The resulting data are now a matrix

$$\widehat{X} = [\widehat{x}_1, ..., \widehat{x}_2] \in \mathbb{R}^{S \times N} \tag{3}$$

with

- $S < min(D, N)$, and
- $x^(i) \in \mathbb{R}^S$ is the i-th sample.

Next the label matrix is constructed in respect to the training matrix $\widehat{X}$ using one-hot encoding[30]. For every training sample $\widehat{x}^{(i)}$ derived from a frequency/class $f \in F$, the label is :

$$\mathbf{y}^{(i)} = [y_1, y_2, ..., y_F]^T, y_j = \begin{cases} 1 & \text{if } j = f \\ 0 & \text{if } j \neq f \end{cases} \tag{4}$$

The resulting label matrix will be: $\mathbf{Y} = [y^{(1)}, ..., y^{(n)}] \in \mathbb{R}^{F \times N}$.
As mentioned before, MLR is aiming to minimize the sum-of-square cost function, the difference between the regressed labels and the actual labels, as follows :

$$min_{W,b} \frac{1}{2} \Sigma_{i=1}^{N} \parallel y^{(i)} - (W^T \widehat{x}^{(i)} + b) \parallel_2^2 \tag{5}$$

where

$$\mathbf{W} = [w_1, w_2, ..., w_C] \in \mathbb{R}^{S \times C}$$

and b is derived by computing the partial derivative of b like :

$$b = \frac{1}{N} \Sigma_{i=1}^{N} (y^{(i)} - W^T \widehat{x}^{(i)})$$

The optimal solution for the weights is given by:

$$W = (\widehat{X}\widehat{X}^T)^{-1} \widehat{X} Y^T$$

Then the weight matrix $\mathbf{W}$ is used for the projection of the training data to the lower dimension. The final feature matrix Z is constructed as follows:

$$Z = W^T \widehat{X} \tag{6}$$

with $Z \in \mathbb{R}^{F \times N}$ and $z^{(i)} \in \mathbb{R}^F$ being the feature vector for each trial.
Regarding the construction of the test feature matrix the procedure is similar. At first the data are mapped to the PCA of the training data and then with the weights W their are projected to the final vector. The whole overview of the procedure can be shown in figure 2.

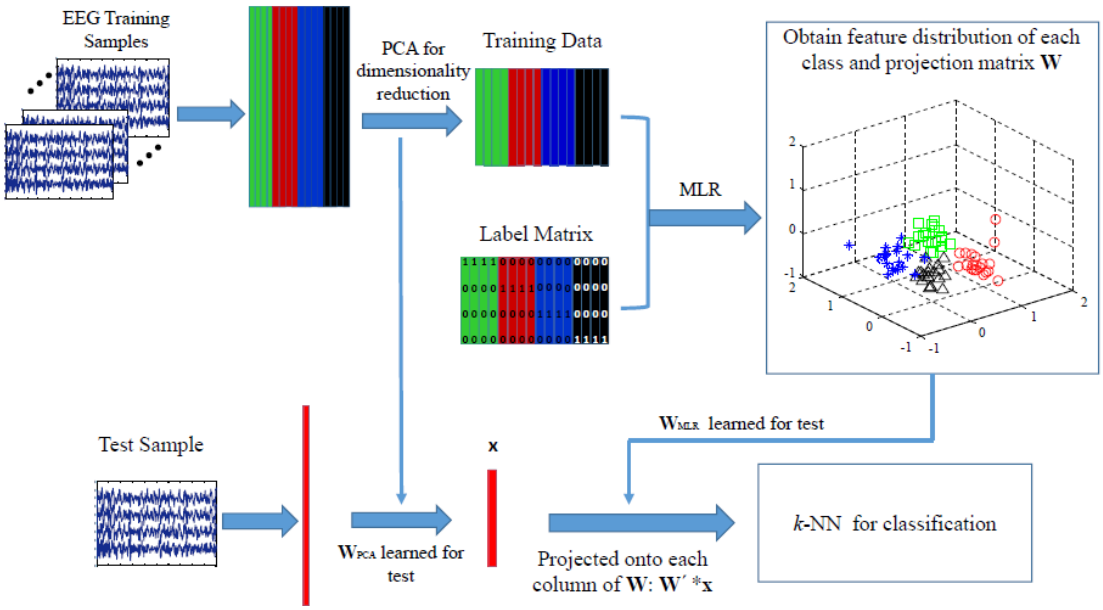

Figure 2: MLR procedure [28]

2.4.2 SSVEP power spectrum

Except of using only the time series we also used the power spectrum as an input to the MLR procedure. The power spectrum was computed using the Fast Fourier Transform (FFT) like:

$$X_f = |FFT(x)|^2 \tag{7}$$

where x is the pre-processed EEG acquired at the calibration phase. Then $X_f in \mathbb{R}^{C \times N}$ and is used as an alternative input to MLR to extract more discriminative features.

2.5 Signal Processing

The gathered EEG signals need to be pre-processed in order to be used, since they are noisy, there have many physiological artifacts and there is a big chance some of the electrodes to not record anything, they have a trend and they need to be re-referenced. The need for pre-processing is vital as our classifier needs to have the best training signals in order to be reliable.

2.5.1 Pre-Processing steps

At first, the data are collected by the buffer and then they are going through the pre-processing steps as follows:

- *detrent*: remove slow drifts and random offsets,
- *remove bad channels*,
- *bad trials*: identify and discard all the outliers,
- *spatial filtering*:Because of the volume conduction, different electrodes in the brain record different magnitudes of the same sources in the brain. For that reason it is required a spatial filtering to decorrelate the sources. The technique that was used was the Common Average Reference (CAR) where the common average of all the electrodes is computed and the it is substructed by the left electrodes.

Spectral Filtering

After the previous processing, the data need to be filtered to allow only the required frequencies, namely the flickering frequencies. For that reason the data are band-pass filtered between the smallest $-1Hz$ or $-2Hz$ and the highest $+1Hz$ or $+2Hz$ frequencies.

Regions of Interest

As it has already been mentioned, the regions that are active during the SSVEP stimuli are the occipital and parieto-occipital areas. For that reason the channels that were used in the analysis were $POz, O1, Oz, O2, P3, Pz, P4, P6, P7$ (figure 3).

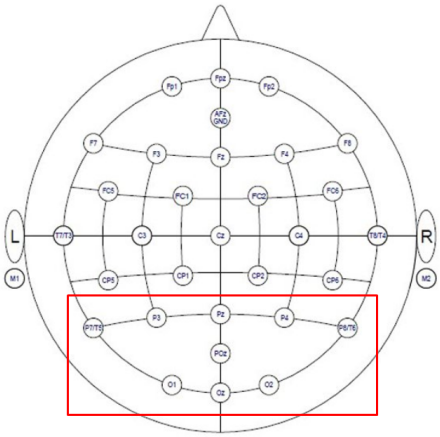

Figure 3: Channel Selection [9]

2.5.2 Training of the classifier

As it was mentioned, in order to train the classifier we used the MLR features. The MLR gives a feature vector $z^{(i)} = [z_1, z_2, .., z_f], i = 1, ..., F$ which is a projection to the $|F|$, every z_i is a component of how close is to a specific flickering frequency. We used two different inputs either the pre-processed time series either the power spectrum. The weight matrices W and principal components were kept to be used in the testing phase. The feature vectors from all the trials used to train a simple classifier, in our case the $k-$Nearest Neighbors[29].

3 Results

For feature extraction of our flickering frequencies $[8.5, 10, 12, 15, 20, 30]Hz$, we filtered the signals between $6 - 32Hz$ and chose the appropriate signals. By using multivariate linear regression, we extracted a feature vector $z = [z_1, z_2, z_3, z_4, z_5, z_6]$ for each trial. Then, we performed $10 - fold$ validation.
We tested our BCI on three different subjects using a k-nearest neighbors algorithm (kNN) with $k = 3$ and a uniform probability distribution for all of the flickering frequencies. Here, we also evaluated the impact of different time window lengths on the classification accuracy. In addition, we compared classification scores between time and frequency domain for this specific setup. Finally, we compared our results with the function `buffer_train_ersp_clsfr.m`[1]. We applied the same frequency band for filtering as well as the CAR technique for the spatial filtering.

Firstly, we used the time-series as an input to MLR, as it was also proposed in [28]. We tried different time windows to see how it influences the classification. The results were really demotivating since the best classification score was acquired using the whole recorded signal, but it didn't achieve high classification score, but rather it was almost a random model (overview of the classification score in Table 2).

Table 2

MLR classification score for time-input in different time windows				
Subjects	1s	2s	3s	4s
1	0.4398	0.5283	0.6062	0.6145
2	0.2975	0.3273	0.3725	0.3788
3	0.4315	0.5808	0.6335	0.6332

After the rather disappointing results we used the frequency spectrum as input to the MLR and extracted the feature vector. The results for Subjects 1 and 3 were very high with Subject 3 achieving almost 99% classification score. However, the data of Subject 3 lead to a model with less than 50% accuracy. Again we used different time windows to compare the optimal windol lengths of recording. Subjects 1 and 3 exhibit more than 85% classification score after 2 seconds. The results can be found in Table 3.

Table 3

MLR classification score for frequency-input in different time windows				
Subjects	1s	2s	3s	4s
1	0.6803	0.8660	0.9162	0.9473
2	0.3472	0.4232	0.4688	0.4905
3	0.7465	0.9653	0.9890	0.9875

In general, the resulting multiple linear regression classification score demonstrate high inter-subject variability. Unsurprisingly, longer time windows seem to increase classification accuracy for the time domain as well as for the frequency domain. Nevertheless, with the exeption of subject 2 the MLR classifier applied on the frequency spectrum outperforms the time domain tremendously.

Interestingly, if the two methods are compared to the ERSP bufferBCI classifier the apparent differences between all three subjects vanish (Table 4).

[1]The function was found in Buffer BCI toolbox.

Table 4

Comparison of different methods			
Subjects	freq→ MLR 2-nn	time → MLR + 2-nn	ERSP buffer clsfr
1	0.9473	0.6145	0.956
2	0.4905	0.3788	1
3	0.9875	0.6332	1

Due to this apparent divergence we evaluated the confusion matrices. It is important to note, that Subject 2 achieves 100% classification score with the buffer BCI function. In contrast, the model created using the MLR features performs worse than random.
As it can be seen in the next figures, regarding Subject 2, it seem that the classes 5 and 6 (each assigned in respect to the flickering frequencies $30Hz$ and 20) cannot be recognized. However, when looking at the power spectrum (Figure 6) we can see that the frequency assigned to class 4, $15Hz$ is a harmonic of the flickering frequency of class 6. The same occurs, for classes 2 and 5, but there doesn't seem to be a comparison. On the other hand, the power spectrum of Subject 1 (figure 5), regarding classes 4,5 and 6, does not seem to have a clear peak in those frequencies. Nevertheless, it's confusion matrix provides high discrimination.

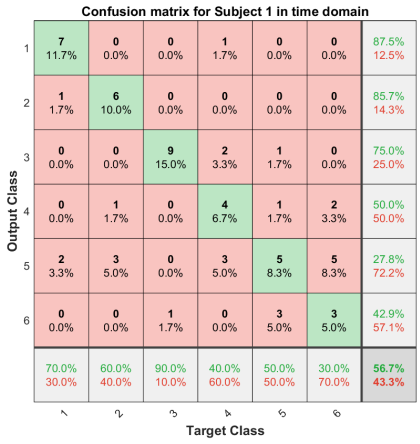

(a) subject 1 - time input

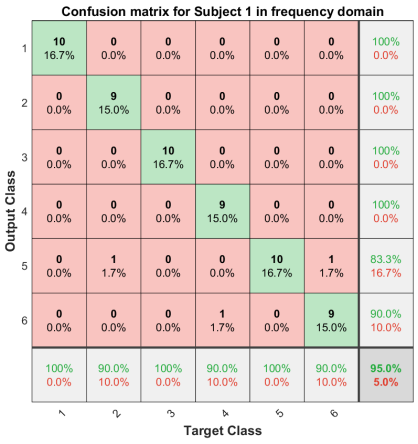

(b) subject 1 - frequency input

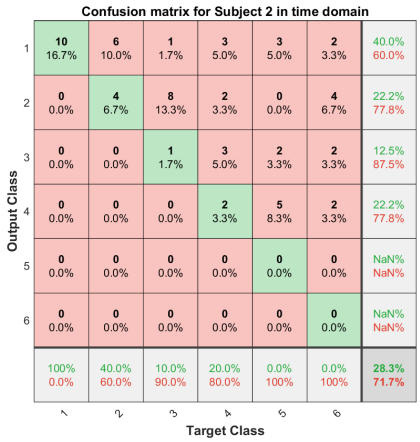

(c) subject 2 - time input

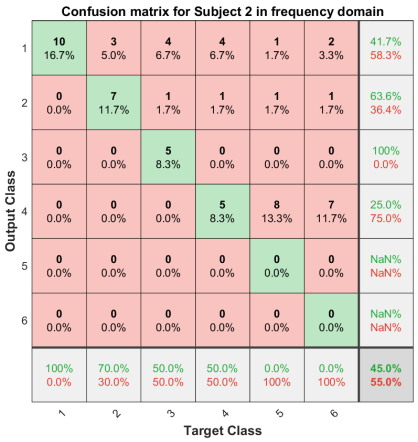

(d) subject 2 - frequency input

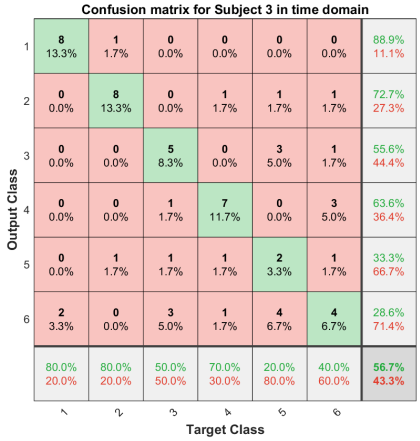

(e) subject 3 - time input

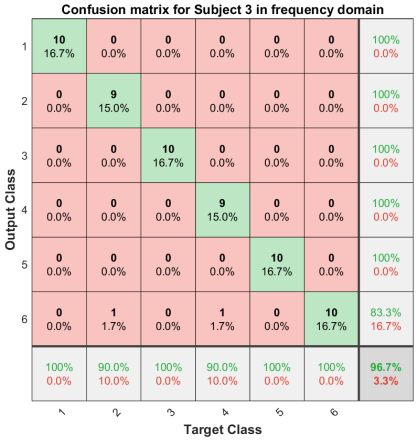

(f) subject 3 - frequency input

Figure 4: Confusion matrices of all the subjects using MLR

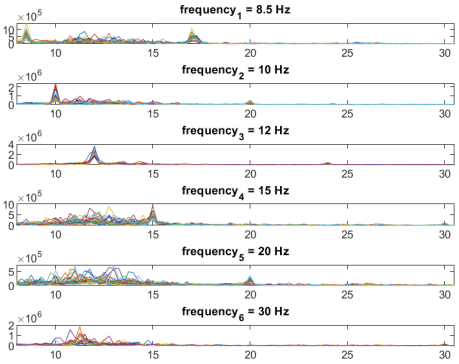

Figure 5: Subject 1

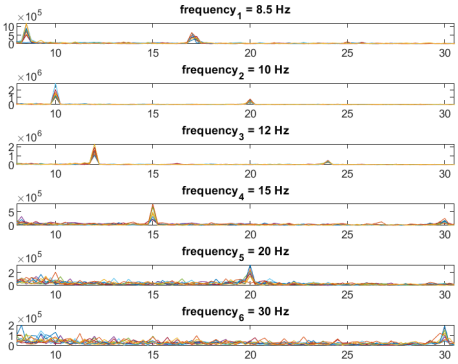

Figure 6: Subject 2

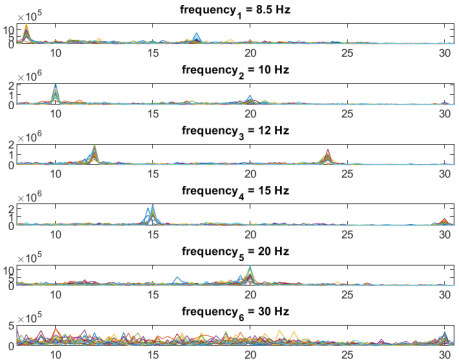

Figure 7: Subject 3

Figure 8: Power spectrum for each class

One of the solutions we came up with was to change the probability distribution in the k-nn classifier, and give a boost to the classes with the least recognition. However, this didn't lead to a better result. When we increased the number of neighbors from $k = 2$ to $k = 3$, the classification score of Subject 2 increased a bit, without exceeding the 60% though.

One of the problems of k-nn is that is prone to over-fitting when you are looking at a big number of neighbors. In our situation, we have feature vectors with length equal to 6 and 20 trials of each class. That means that we cannot use a big number of neighbors.

4 Discussion

In this report we present our SSVEP based BCI. We created a brain computer interface that uses brain signatures from the visual pathway as a result of visual entrainment of different flickering frequencies. We developed our own processing pipeline consisting of pre-processing and data analysis. We utilized a multiple linear regression classifier using a k- nearest neighbour algorithm. Our initial idea included next to the SSVEP imagined movement and alpha waves as brain signals for different functionality. During our first testing sessions, we realized that the alpha waves and imagined movement proved themselves very challenging. As a result we focused on SSVEP. One of the reasons why alpha waves lead to very low classification accuracies in our classifier were the very low signal to noise ratio inherent in our alpha activity. Discarding the alpha waves classes from our training data led to immediate improvements in classification accuracy. Hence, we excluded the alpha waves in our finalized version. Similarly, the imagined movement classes showed less clear signal spectra compared to the SSVEP response. This was unsurprising, considering the aforementioned accuracy differences between different BCI paradigms. As a consequence, we adapted our menu and used SSVEP for our sub-tasks and menu switching.

Even though we reduced ourselves on the steady state visual evoked potential during demonstration day our system produced erroneous decisions. Here, we tested for several scenarios to find the reasons contributing to the outcome:
Firstly, we checked for overfitting between training and test data using cross validation. We partitioned the sample data into complementary subsets and tested them against each other. The resulting accuracies were high and did not show high variability between partitions. Then, we used decreasingly small subsets of our training data (e.g. 30%) to predict the remaining data (70 %). Again, our classifier achieved high precision. Hence, we believe overfitting did not contribute to the training - test disparity.
Secondly, we checked our frequencies and adjusted them accordingly. Here, we tried to increase the difference between frequency peaks to avoid overlap within the spectrum and possible confusion. Again, our classifier accuracies were high. In addition, the confusion matrices demonstrate a substantial difference between the time and the frequency domain. One explanation to this divergence might lay in the hardware used in our setup. We experienced several connection failures, where the Mobita system either disconnected during calibration or the system appeared to be frozen for short amounts of time. Whenever we found out about it, we discarded the data. However, undiscovered, tiny lags in the time domain due to connection issues can lead to big consequences. However, in theory those lags are resolved in the frequency domain without much of an effect. Nevertheless, even with high differentiability between classes in the frequency spectra our system could not correctly identify many test trials in the testing phase.
Thirdly, we adapted the probability distribution of each class manually to achieve a better testing during the feedback phase. Here, we used different weighting factors to balance the classification certainty between classes. Nevertheless, the classifier preferentially selected a few specific erroneous classes.
Lastly, we changed the number of neighbors during classifier training. Doing so increased the risk of overfitting but it did not change the outcome during the testing session.

We believe, several solutions can be implemented to increase positive classifications during our testing of the BCI. One potential solution to our problem might lay in transfer learning. The apparent differences between training and testing might be due to a variety of dynamics that either changed the mean offset or the feature orientations in feature space.
Another solution might be that our choice of classification using kNN and MLR are either unsuited for the data or not correctly implemented. This argumentation could explain the differences in classifier accuracy between our classifier and the ERSP classifier from the buffer BCI.
In addition, our choice of frequencies contains a variety of shared harmonics and sub-harmonics. Some frequencies are multiples of each other. This could lead to a diminished signal to noise ratio during testing, where the user might be less focused than during the calibration phase.

Furthermore, we could improve our system using canonical correlation analysis (CCA), which has been shown to work very well with SSVEP BCI's. We tried to implement CCA but did not succeed to construct suitable reference signals. Here, features within the signal are extracted by calculating the correlation between the signal and a constructed reference signal. Doing so could also lead to shorter calibration times with higher accuracy.

5 Conclusion

We put a lot of effort in creating the whole system from scratch. In addition, we implemented many different classification pipelines to accommodate for the rather dissatisfying results acquired during the practice sessions.

References

[1] Laura J. Ball, David R. Beukelman, and Gary L. Pattee. "Acceptance of augmentative and alternative communication technology by persons with amyotrophic lateral sclerosis". In: *AAC: Augmentative and Alternative Communication* 20.2 (2004), pp. 113–122. ISSN: 07434618. DOI: 10.1080/07434610420002165 96.

[2] Ali Bashashati et al. "A survey of signal processing algorithms in brain–computer interfaces based on electrical brain signals". In: *Journal of Neural engineering* 4.2 (2007), R32.

[3] Chris Bonnell. "Kuramoto Oscillators". In: (2011), pp. 1–8.

[4] J. K. Bowmaker. "Trichromatic colour vision: why only three receptor channels?" In: *Trends in Neurosciences* 6.C (1983), pp. 41–43. ISSN: 01662236. DOI: 10.1016/0166-2236(83)90019-X.

[5] Pietro Cipresso et al. "The use of P300-based BCIs in amyotrophic lateral sclerosis: From augmentative and alternative communication to cognitive assessment". In: *Brain and Behavior* 2.4 (2012), pp. 479–498. ISSN: 21623279. DOI: 10.1002/brb3.57.

[6] Joseph Classen et al. "Integrative Visuomotor Behavior Is Associated With Interregionally Coherent Oscillations in the Human Brain". In: *Journal of Neurophysiology* 79.3 (2017), pp. 1567–1573. ISSN: 0022-3077. DOI: 10.1152/jn.1998.79.3.1567.

[7] Gerald Cooray. "The Kuramoto Model". In: *Leonardo* September (2008). URL: http://www.mendeley.com/research/kuramoto-model/.

[8] Anna Duszyk et al. "Towards an optimization of stimulus parameters for brain-computer interfaces based on steady state visual evoked potentials". In: *PLoS ONE* 9.11 (Nov. 2014). ISSN: 19326203. DOI: 10.1371/journal.pone.0112099.

[9] *EEG cap from mobita*. https://www.biopac.com/product/h2o-caps-for-mobita-wireless-eeg/. Accessed: 2019-06-27.

[10] Berger Hans. "Electroencephalogram in humans". In: *Archiv für Psychiatrie and Nervenkrankheiten* 278.1875 (1929), 87: 527- 570. ISSN: 0003-9373. DOI: 10.1007/BF01797193. URL: http://link.springer.com/10.1007/BF01797193.

[11] C. S. Herrmann. "Human EEG responses to 1-100 Hz flicker: Resonance phenomena in visual cortex and their potential correlation to cognitive phenomena". In: *Experimental Brain Research* 137.3-4 (2001), pp. 346–353. ISSN: 00144819. DOI: 10.1007/s002210100682.

[12] Netiwit Kaongoen and Sungho Jo. "A novel hybrid auditory BCI paradigm combining ASSR and P300". In: 279 (2017), pp. 44–51.

[13] J. D. Kropotov. "Type of Beta Rhythms". In: *Quantitative EEG, Event-Related Potentials and Neurotherapy* (2009), pp. 59–76.

[14] Asier Lopez-Basterretxea, Amaia Mendez-Zorrilla, and Begoña Garcia-Zapirain. "Eye/head tracking technology to improve HCI with iPad applications". In: *Sensors (Switzerland)* 15.2 (2015), pp. 2244–2264. ISSN: 14248220. DOI: 10.3390/s150202244.

[15] J R Mill et al. "Asynchronous Non-Invasive Brain-Actuated Control of an Intelligent Wheelchair". In: (), pp. 3–6.

[16] Gernot R. Müller-Putz and Gert Pfurtscheller. "Control of an electrical prosthesis with an SSVEP-based BCI". In: *IEEE Transactions on Biomedical Engineering* 55.1 (2008), pp. 361–364. ISSN: 00189294. DOI: 10.1109/TBME.2007.897815.

[17] Christoph Neuwirth and Markus Weber. "UNMASKING THE SILENT MOTOR NEURON LOSS IN AMYOTROPHIC LATERAL SCLEROSIS". In: August (2018), pp. 184–185. DOI: 10.1002/mus.26134.

[18] Mehdi Ordikhani-Seyedlar. *What happens in your brain when you pay attention?* 2017. URL: https://www.ted.com/talks/mehdi_ordikhani_seyedlar_what_happens_in_your_brain_when_you_pay_attention?utm_campaign=tedspread&utm_medium=referral&utm_source=tedcomshare.

[19] Jobin T. Philip and S. Thomas George. "Visual P300 Mind-Speller Brain-Computer Interfaces: A Walk Through the Recent Developments With Special Focus on Classification Algorithms". In: *Clinical EEG and Neuroscience* (2019). ISSN: 21695202. DOI: 10.1177/1550059419842753.

[20] John Polich. "Subject : Experience Letter". In: 118.10 (2017), p. 1999. DOI: 10.1016/j.clinph.2007.04.019.Updating.

[21] Yunyong Punsawad, Student Member, and Yodchanan Wongsawat. "Hybrid SSVEP-Motion Visual Stimulus based BCI System for Intelligent Wheelchair". In: *2013 35th Annual International Conference of the IEEE Engineering in Medicine and Biology Society (EMBC)* (2013), pp. 7416–7419. DOI: 10.1109/EMBC.2013.6611272.

[22] Hikaru Sato and Yoshikazu Washizawa. "An N100-P300 Spelling Brain-Computer Interface with Detection of Intentional Control". In: (2016), pp. 1–20. DOI: 10.3390/computers5040031.

[23] Stefano Silvoni et al. "Amyotrophic lateral sclerosis progression and stability of brain-computer interface communication of brain-computer interface communication". In: 8421 (2013). DOI: 10.3109/21678421.2013.770029.

[24] Samuel G. Solomon and Peter Lennie. "The machinery of colour vision". In: *Nature Reviews Neuroscience* 8.4 (2007), pp. 276–286. ISSN: 1471003X. DOI: 10.1038/nrn2094.

[25] P. K. Stanton et al. "A human intracranial study of long-range oscillatory coherence across a frontal-occipital-hippocampal brain network during visual object processing". In: *Proceedings of the National Academy of Sciences* 105.11 (2008), pp. 4399–4404. ISSN: 0027-8424. DOI: 10.1073/pnas.0708418105.

[26] Matteo Toscani et al. "Alpha waves: A neural signature of visual suppression". In: *Experimental Brain Research* 207.3-4 (2010), pp. 213–219. ISSN: 00144819. DOI: 10.1007/s00221-010-2444-7.

[27] S. Vanni et al. "Retinotopic distribution of chromatic responses in human primary visual cortex". In: *European Journal of Neuroscience* 24.6 (2006), pp. 1821–1831. ISSN: 0953816X. DOI: 10.1111/j.1460-9568.2006.05070.x.

[28] Haiqiang Wang et al. "Discriminative feature extraction via multivariate linear regression for SSVEP-based BCI". In: *IEEE Transactions on Neural Systems and Rehabilitation Engineering* 24.5 (2016), pp. 532–541.

[29] Wikipedia contributors. *K-nearest neighbors algorithm — Wikipedia, The Free Encyclopedia*. https://en.wikipedia.org/w/index.php?title=K-nearest_neighbors_algorithm&oldid=899016278. [Online; accessed 27-June-2019]. 2019.

[30] Wikipedia contributors. *One-hot — Wikipedia, The Free Encyclopedia*. https://en.wikipedia.org/w/index.php?title=One-hot&oldid=895603798. [Online; accessed 27-June-2019]. 2019.

[31] Zhenghua Wu. "Physical connections between different SSVEP neural networks". In: *Scientific Reports* 6.April 2015 (2016), pp. 1–9. ISSN: 20452322. DOI: 10.1038/srep22801. URL: http://dx.doi.org/10.1038/srep22801.